Advanced Swing Leg Control for Stable Locomotion

Yvonne Blum, Juergen Rummel and Andre Seyfarth

Locomotion Laboratory, University of Jena, Germany,
yvonne.blum@uni-jena.de,
www.lauflabor.de

Abstract Locomotion can be described as a subsequent series of stance and flight phases. In both phases the leg properties can be adapted. Here we consider spring-mass running with a linear adaptation of two leg parameters, leg angle and leg stiffness, during swing phase. The region of stability is characterized by the basin of attraction with sufficient reduction of a given perturbation within one step.
The proposed swing-leg control predicts a substantial region of alternative swing leg adjustment rates. The resulting control redundancy includes different foot placement strategies which could be used to manage landing impacts and running stability in one consistent approach.

1 Introduction

Due to its simplicity and its explanatory power, the spring-mass model is an adequate mechanical template to describe bouncing gaits like running, jumping or hopping. Here, the complex structure of a human leg is simplified by a linear spring attached to a point mass representing the body's center of mass [1].

For given system energy steady state locomotion can be described based on three leg parameters: the angle of attack, the leg stiffness and the rest length of the leg. For proper adjustments of these parameters and speeds higher than 3.5 m/s self-stable locomotion is found [2]. Here we ask, to what extent the region of stable running can be enlarged (e.g. to include lower speeds) by adapting the leg parameters during swing phase. It has been previously shown that running at low speeds can be stabilized by employing leg retraction prior to contact [3].

In human and animal locomotion leg stiffness can be adjusted by the neuromuscular system. Similar adjustments of elastic properties have already been implemented in technical legs [4]. In the present study we propose a linear stiffness change of the leg during swing phase in addition to swing-leg retraction. For periodic running (satisfying constant apex heights of two subsequent flight phases) we consider combinations of constant leg stiffness and leg angle rates that guarantee stable locomotion over a large range of speeds. The identified combintions of both swing-leg control strategies can be used in legged robots based on compliant leg behavior.

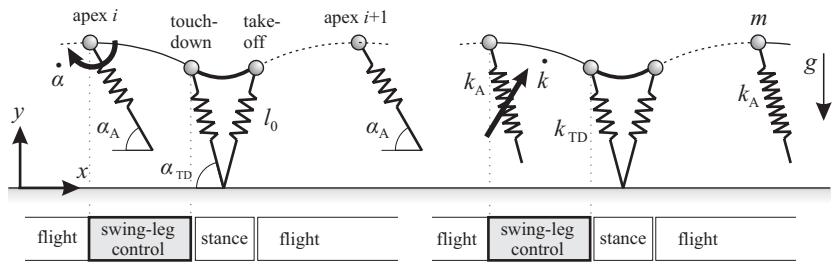

Figure 1. The spring-mass model for running with two swing-leg control strategies: leg rotation (left) and stiffness adaptation of the leg spring (right).

2 Methods

Model: The planar spring-mass model is characterized by alternating flight and stance phases (Figure 1). The body is represented as a point mass which is, during stance, influenced by gravity $\boldsymbol{g}$ and a force exerted by the leg spring (stiffness k_{TD}, rest length l_0) attached. The equation of motion is

$$m\ddot{\boldsymbol{r}} = k_{\mathrm{TD}} \left(\frac{l_0}{|\boldsymbol{r}|} - 1 \right) \boldsymbol{r} - m\boldsymbol{g}, \tag{1}$$

where $\boldsymbol{r} = (x, y)$ is the position of the center of mass. If the length of the massless spring reaches its rest length, the system changes into flight phase and describes a ballistic curve. Touch-down occurs if the landing condition $y \leq l_0 \sin(\alpha_{\mathrm{TD}})$ is satisfied. Since the system is conservative and the ground is even the systems state during flight can be fully described by the horizontal velocity v_{X} and the apex height y_{A}, which is the upper point where the vertical velocity v_{Y} equals zero. In this paper, we define the system energy $E = m\,g\,y_{\mathrm{A}} + m/2\ v_{\mathrm{X}}^2$ by choosing a reference velocity $v_{\mathrm{X,REF}}$ and an apex height of $y_{\mathrm{A}} = l_0$. The model parameters are mass $m = 80\,\mathrm{kg}$, leg length $l_0 = 1\,\mathrm{m}$, and gravitational acceleration $g = 9.81\,\mathrm{m/s^2}$.

System analysis: The running system can be analyzed using a return map of the state vector. A one-dimensional return map of two subsequent apex heights $y_{\mathrm{i+1}}(y_{\mathrm{i}})$ can be used to describe the system's stability. Periodic running requires a solution where $y_{\mathrm{i+1}} = y_{\mathrm{i}}$, indicating a fixed point y^* in the apex return map. Stability of the periodic movement can be identified using the slope s in the neighborhood of the fixed point

$$s = \left. \frac{dy_{\mathrm{i+1}}}{dy_{\mathrm{i}}} \right|_{y^*}, \tag{2}$$

where the condition $|s| < 1$ must be fulfilled. A zero slope indicates superstable running where small perturbations will be completely compensated after one step. A stable fixed point has a basin of attraction which is limited (i) by an

apex-height y_{i+1} lower than the landing condition $l_0 \sin(\alpha)$, (ii) by potential energy $m\,g\,y_{\mathrm{i}}$ higher than the system energy E, and (iii) by a second fixed point.

To characterize how fast the system returns to the stable solution after perturation, we start the simulation at the perturbed apex $y_{\mathrm{i}} = y^* + y_{\mathrm{P}}$ (apex condition: $v_{\mathrm{Y}} = 0$), where y_{P} is a small deviation of magnitude 0.001 m and 0.05 m. The horizontal velocity v_{X} is adapted such that the system energy remains constant. Now the slope can be calculated approximately as the difference quotient $s = \left(y_{\mathrm{i+1}} - y^*\right)/y_{\mathrm{P}}$.

Control strategy: The swing-leg control, proposed here, intends to adapt the leg parameters leg angle α and leg stiffness k during the second half of flight phase, starting at the instant of apex t_{A}. The parameters will be adapted using constant rates of change $\dot{\alpha}$ and $\dot{k}$

$$\alpha(t) = \alpha_{\mathrm{A}} + \dot{\alpha} \cdot (t - t_{\mathrm{A}}) \tag{3}$$

$$k(t) = k_{\mathrm{A}} + \dot{k} \cdot (t - t_{\mathrm{A}}). \tag{4}$$

The parameters at apex α_{A} and k_{A} are chosen such that for given rates the touch-down values α_{TD} and k_{TD} equal the constant parameters of a previously found periodic solution $\alpha_{\mathrm{A}} = \alpha_{\mathrm{TD}} - \dot{\alpha} \cdot t_{\mathrm{F}}/2$ and $k_{\mathrm{A}} = k_{\mathrm{TD}} - \dot{k} \cdot t_{\mathrm{F}}/2$, respectively. The time $t_{\mathrm{F}}/2$ corresponds to the duration remaining from apex to touch-down obtained from the apex height y_{A} of the periodic solution $(t_{\mathrm{F}}/2)^2 = 2/g\,(y_{\mathrm{A}} - l_0 \sin \alpha_{\mathrm{TD}})$. The swing-leg control ends at touch-down and during stance the leg stiffness is constant k_{TD}.

3 Results

We first have to find steady state running for a given parameter set. The apex heights of periodic running are mapped for a constant leg stiffness k and a number of system energies E in Figure 2(a), and for varying stiffness at one energy level in Figure 2(b). Many solutions for cyclic running result for given energies or given leg stiffness. In both cases an adequate angle of attack can be found to achieve equal apex heights of two subsequent steps. With increasing leg angles a lower system energy (Figure 2(a)) or a higher leg stiffness (Figure 2(b)) is needed to achieve a periodic solution at the same apex height. It also becomes clear that, aiming at constant apex height, the duration of the flight phase lenghtens with leg softening (Figure 2(b)).

To demonstrate results for the proposed swing-leg strategies, one solution of periodic running has been selected. We choose a reference velocity of 2.5 m/s and a leg stiffness of 20 kN/m, typically observed in human running [3]. Then we calculate the apex height and angle of attack such that the time $t_{\mathrm{F}}/2$ remaining from apex to touch-down is 50 ms (see Table 1). This solution is found to be unstable without control, with a slope s greater than one ($s = 1.69$).

Figure 3 shows not only one but many combinations of stiffness change and retraction leading to superstable running ($s = 0$)) for small perturbations. Moreover, a linear relationship between both parameters is found. The control strategies $\dot{k}$ and $\dot{\alpha}$, are replaceable since a rate of stiffness change exists for zero leg

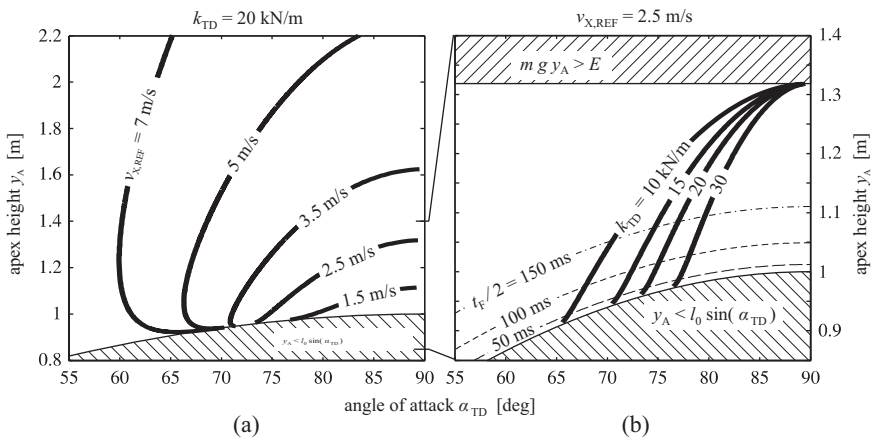

Figure 2. Apex heights of steady state running solutions in the spring-mass model: (a) for constant leg stiffness k_{TD} and various system energies E (represented by reference velocities $v_{\mathrm{X,REF}}$), and (b) for constant system energy E. Each point on the thick lines represents a fixed point in the apex return map. The thin lines in (b) show the apex height corresponding to the time $t_{\mathrm{F}}/2$ remaining from apex to touch-down. During this time the advanced swing-leg control is applied.

rotation ($\dot{\alpha} = 0$) resulting in a superstable running pattern and vice versa. We call these values the optimal rate of stiffness change $\dot{k}_{\mathrm{OPT}}$, respectively optimal speed of leg rotation $\dot{\alpha}_{\mathrm{OPT}}$ (see Table 1 for numerical values).

Beside the optimal control, it is important to know how accurately the swing-leg control has to be tuned for adequate stabilization. Herefore, we demand the resultant slope to lie within $s = (-0.5, 0.5)$. Thus, a small perturbation will be at the worst bisected after one running step. Figure 3 shows the resultant region of moderate control settings which lies left and right along the line for superstable control. This region linearly widens with increasing change of stiffness and increasing leg retraction speed. The width of the mentioned $s = (-0.5, 0.5)$ region is found to be relatively large (e.g. for $\dot{k} = \dot{k}_{\mathrm{OPT}}/2$ the leg should retract with a speed $\dot{\alpha}$ between 19 and 79 deg/s). Hence, the swing-leg controller does not need to be specifically adjusted for stable running.

The swing-leg control is also tested for larger perturbations, $y_{\mathrm{P}} = 0.05\,\mathrm{m}$ (Figure 3, dashed lines). For swing-leg retraction ($\dot{\alpha} > 0$) similar results compared to smaller perturbations can be observed, whereas for a protracting leg the regions of stabilization differ from each other. We examine this difference using the apex return maps shown in Figure 4. The solutions (b), (c), and (d) are selected from the $s = 0$ line in Figure 3 and generate a dead-beat control for small perturbations. The mappings (b) and (d) have a positive slope for higher apices and longe distance from the diagonal, originating from control settings with leg retraction. The mentioned properties of the return map are good to stabilize large dirsturbances as exemplary shown in the mapping (d) where a

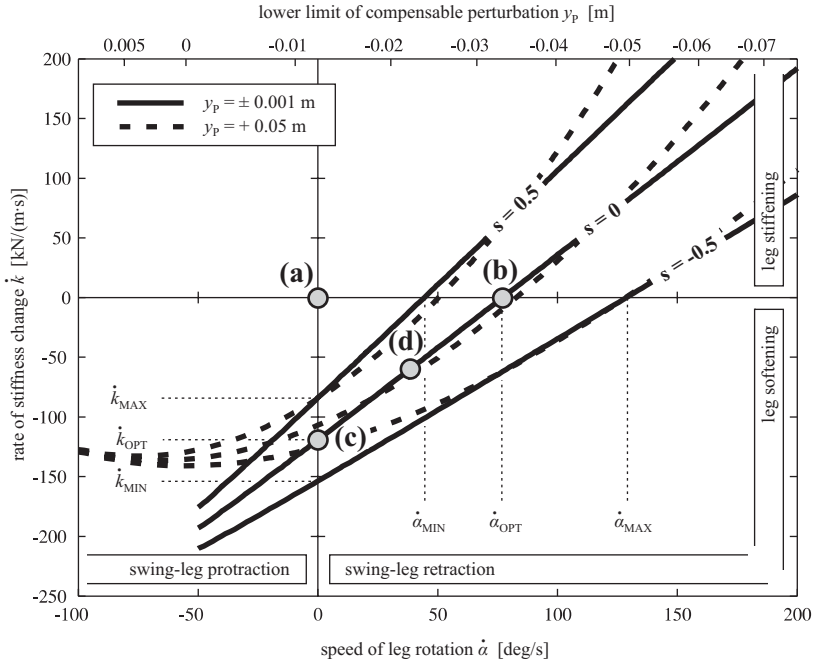

Figure 3. Stability of one periodic running solution (first row in Table 1) dependent on swing-leg control $\dot{\alpha}$ and $\dot{k}$. The quality of stabilization is illustrated by the slope s near the fixed point in the apex return map for small perturbations (thick solid lines) and one larger disturbance (thick dashed lines). The top axis shows how large a negative perturbation can be, dependent on leg rotation $\dot{\alpha}$, such that the runner doesn't stumble.

perturbation of $y_P = 0.227\,\mathrm{m}$ ($y_i = 1.2\,\mathrm{m}$) is compensated after three running steps. The control for optimal change of stiffness ($\dot{k} = \dot{k}_{OPT}$ and $\dot{\alpha} = 0$) generates a negative slope for larger perturbations and the system could stumble after one step. As shown in Figure 4(c), the basin of attraction for compensating pertubations is very restricted compared to the solutions with leg retraction. Hence, for stabilizing larger perturbations the single swing-leg strategies are not exchangeable but a combination of both (d) produces advantageous stability in running. Furthermore, the basin of attraction shifts to greater negative values of perturbations with increasing retraction speed (see top axis in Figure 3). Since the faster retraction starts with a smaller leg angle α_A the ground clearance increases and the stumble limit decreases to lower apices.

4 Discussion

In this paper, we proposed a conceptual method for stabilizing running and tested it with the spring-mass model. The method is divided into two parts,

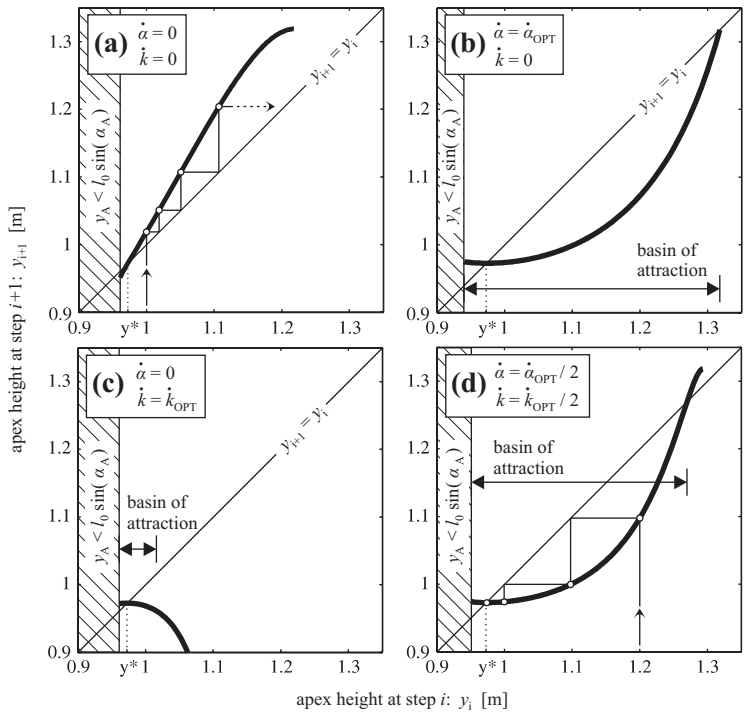

Figure 4. Return maps of the apex height $y_{i+1}(y_i)$ for the same periodic running solution (first row in Table 1) and some swing-leg strategies. The graphs correspond to the parameter combinations selected in Figure 3.

the swing-leg retraction and the stiffness adaptation, which are both suffient for stabilization of existing periodic running solutions. We have shown that the leg retraction is not a unique method while it seems to be essential for successful legged locomotion [6]. However, in experiments on human running [5] a mean retraction speed of $\dot{\alpha} = 44\,\mathrm{deg/s}$ has been measured which is much lower than the model predicted values for optimal stabilization ($\dot{\alpha}_{\mathrm{OPT}} = 77 - 104\,\mathrm{deg/s}$) at related conditions. This let us assume that further control strategies are used to improve locomotion. The change of leg stiffness during flight could be one of them where a dead-beat control can be observed for small perturbations. Although, the stiffness adaptation alone is largely limited in compensating disturbances, in a combined control it might help to reduce the required rotational speed (Figure 3). Assuming a non-massless leg, the running system could then be stabilized with a lower amount of forces and probably higher energy efficiency.

The proposed control strategy intends to adapt the leg stiffness during flight with the leg becoming softer with increasing flight time. However, the stiffness adaptation, respectively the leg softening, could also be done during stance phase. This possibility was discovered in segmented legs as passive built-in mechanism resulting in improved stability compared to the spring-mass model [7].

Table 1. Selected periodic running solutions and parameters for optimal swing-leg control and limitations. The last row contains human data [5].

properties of the periodic solution					swing-leg control					
$v_{\mathrm{X,REF}}$ [m/s]	$t_{\mathrm{F}}/2$ [ms]	y_{A} [m]	k_{TD} [kN/m]	α_{TD} [deg]	$\dot{\alpha}_{\mathrm{MIN}}$	$\dot{\alpha}_{\mathrm{OPT}}$ [deg/s]	$\dot{\alpha}_{\mathrm{MAX}}$	$\dot{k}_{\mathrm{MIN}}$	$\dot{k}_{\mathrm{OPT}}$ [kN/(m·s)]	$\dot{k}_{\mathrm{MAX}}$
2.5	50	0.973	20	73.8	44	77	129	-154	-119	-84
2.5	100	1.015	20	75.1	62	104	159	-249	-191	-132
5.0	50	0.940	20	68.1	-24	-9	22	-17	11	39
5.0	100	0.968	20	66.8	2	27	60	-67	-35	-3
2.7	23	1.017	25	73.7	9	44	79	n/a		

The here investigated model is limited in compensating negative perturbations, respectively running a step upward (Figure 4). If a running system has to deal with very uneven ground it could choose a periodic solution with a higher apex enhancing the ground clearance. However, since the rate of changes of the leg parameters need to be higher (Table 1), this option might be disadvantagous. Another possibility for successful running on largely uneven ground was experimentally observed as the adaption of leg length [8,9]. Taken into account that the nominal length of a segmented leg is an easy changeable parameter, a length adjustment of the leg could also enhance running stability. Investigations on this topic remain for future studies to further advance the swing-leg control.

Acknowledgements

This study is supported by the German Research Foundation (DFG, SE1042).

References

1. Blickhan R: The Spring-mass Model for Running and Hopping. J Biomech **22**: 1217-1227, 1989
2. Seyfarth A, Geyer H, Guenther M, Blickhan R: A Movement Criterion for Running. J Biomech, **35**: 649-655, 2002
3. Seyfarth A, Geyer H, Herr H: Swing-leg Retraction: a Simple Control Model for Stable Running. J Exp Biol **206**: 2547-2555, 2003
4. Van Ham R, Vanderborght B, Van Damme M, et al.: MACCEPA: The Actuator with Adaptable Compliance for Dynamic Walking Bipeds. CLAWAR, 2005
5. Lipfert S, Seyfarth A: How similar are walking and running? (in prep.)
6. Herr HM, McMahon TA: A Galloping Horse Model. Int J Robot Res **20**: 26-37, 2001
7. Rummel J, Seyfarth A: Stable Running with Segmented Legs. Int J Robot Res (submitted)
8. Blickhan R, Seyfarth A, Geyer H, et al.: Intelligence by Mechanics. Phil Trans R Soc A **365**: 199-220, 2007
9. Daley MA, Felix G, Biewener AA: Running Stability Is Enhanced by a Proximo-distal Gradient in Joint Neuromechanical Control. J Exp Biol **210**: 383-394, 2007